Russian Journal of Earth Sciences

Investigation of Tidal and Subtidal Variations in Sea Level Close to the Southeastern Coast of Sakhalin Island Using Two-Year Time Series

Dmitry Kovalev[1], **Andrey Kurkin**[*2], **Peter Kovalev**[1] **and Vitaly Zarochintsev**[1]

[1] Institute of Marine Geology and Geophysics Far Eastern Branch Russian Academy of Sciences, Yuzhno-Sakhalinsk, Russia
[2] Nizhny Novgorod State Technical University n.a. R. E. Alekseev, Nizhny Novgorod, Russia
* **Correspondence to:** Andrey Kurkin, aakurkin@gmail.com.

Abstract: The results of the study of tidal and subtidal variations in sea level in the area of the southeastern coast of the Sakhalin Island and a series of atmospheric pressure and wind speed from the open website "Weather Schedule" are presented. Using spectral analysis, astronomical tides were studied and diurnal M_1, K_1 and semi-diurnal M_2, S_2 tidal harmonics with high energy were detected. The maximum heights of tidal waves have been determined and the tidal regime in the studied water area is classified as mixed with a predominance of diurnal tides. It is shown that sea level rises due to the impact of winds on the sea surface are observed in the northerly direction of the winds, which is associated with storm surge in the coastal zone of Mordvinov Bay. The lowering of the sea level is observed with southerly winds and it is caused by the downsurge. The magnitude of the decrease in sea level for events that have a correlation between high wind speeds and the duration of influence to the winds of the western directions is maximal, and the wind speed has less influence on the magnitude of the decrease in level than its duration. Calculations of the level response to changes in atmospheric pressure using the Proudman equation and analysis of the results showed that these events can be attributed to the phenomenon of the "inverted barometer". A comparison of theoretical profiles calculated from the time form of the Korteweg–de Vries equation with the registered profiles of sea level showed that they are well described by the profile of a solitary wave.

Keywords: sea level variations, tidal waves, wave set-up, storm surge and downsurge, inverted barometer, cnoidal wave.

Citation: Kovalev, D., A. Kurkin, P. Kovalev and V. Zarochintsev (2024), Investigation of Tidal and Subtidal Variations in Sea Level Close to the Southeastern Coast of Sakhalin Island Using Two-Year Time Series, *Russian Journal of Earth Sciences*, 24, ES3001, EDN: EHYHPC, https://doi.org/10.2205/2024es000908

1. Introduction

The study of sea level variations due to waves is carried out in many marine areas, since knowledge of their parameters is necessary for practical purposes such as navigation, fishing and mining on the shelf. At the same time, the range of studied periods of these processes is quite wide – from a few seconds to several tens of days, although waves in the range from wind waves to diurnal tidal waves are more often analyzed.

At the same time, the mechanism of sea level fluctuations on time scales from tidal to several days has been little studied [*Andrade et al.*, 2018], which is due to the scarcity of observational data duration several hundred days and there are a small number of papers with the results of studying processes with time scales longer days [*Andrade et al.*, 2018; *Truccolo et al.*, 2006]. This makes it impossible to determine the forces causing sea level oscillations. In addition, the time series of sea level oscillations analyzed in the paper [*Andrade et al.*, 2018] showed that the maximum amplitude of such long-period oscillations is quite large and, when combined with spring tide, can lead to extreme events of sea level rise on the coast, which represents a direct threat to coastal human habitats and

Research Article

Received: 3 February 2024
Accepted: 2 April 2024
Published: 13 June 2024

has repeatedly occurred, for example, on the western coast of the Kamchatka Peninsula [*Kovalev et al.*, 1991].

It should be noted that there are quite a large number of papers on monitoring sea level changes near coasts in different areas of the World Ocean, for example, [*Pérez Gómez et al.*, 2022; *Valentim et al.*, 2013; *Williams*, 2013] but the observations obtained from these studies are used to analyze coastal erosion or to monitoring sea level changes associated with climate change and possible coastal flooding. In the recent paper [*Koohestani et al.*, 2023] the authors analyzed the appearance of internal solitary waves in the Bay of Oman caused different mechanisms including variations of atmospheric pressure, wind, currents, etc. Note also two more publications that relate to the study of long-term changes in sea level and the identification of a trend in rising sea levels [*Goryachkin et al.*, 1999; *Raj et al.*, 2022]. Among domestic authors, we note investigations with the participation of E. G. Morozov to study the temporal and spatial variability of hydrological processes and internal waves in a wide range of scales, such as, for example, [*Morozov et al.*, 2020].

Also, it is of interest what the magnitude of astronomical tides is in the water area under consideration, since they are often not considered or overlooked due to their small magnitude, or the lack of long-term time series data. This does not allow us to determine the actual forces that drive sea level oscillations with periods greater than daily in the coastal zone. In addition, understanding and dissociating long-period oscillations caused by astronomical and meteorological forcing is very important for navigation safety, coastal engineering, sedimentation studies and other factors.

Study of sea level oscillations in the southeastern part of the Sakhalin Island are conducted for many years using autonomous wave meters. The research results have been published in several papers, for example, [*Kovalev et al.*, 2022; *Kovalev and Kovalev*, 2018; *Kurkin et al.*, 2023; *Squire et al.*, 2021a]. However, the analysis of level oscillations with time scales longer than tidal was carried out in only one paper [*Kovalev et al.*, 2022], but time series duration several months were used. In addition, analysis of time series duration 700 days makes it possible to clarify the periods of astronomical sea level oscillations.

Despite the fact that the Laboratory of Wave Dynamics and Coastal Currents of the Institute of Marine Geology and Geophysics, Far Eastern Branch of the Russian Academy of Sciences, carried out year-round observations of sea level oscillations near the settlement Okhotskoe, south-eastern coast of the Sakhalin Island, the obtained time series were not always continuous with the annual change of recording devices. It was possible to select only one continuous time series with a duration of 700 days, which was used for research. Note that this work mainly considers the results of the analysis of the astronomical tide and level variations as a result of the influence of atmospheric disturbances.

2. Observations

Wave observations were carried out using autonomous wave recorders ARW-10 and ARW-14 with serial number 32 in 2015, number 109 in 2015–2016 and 94 in 2016–2017. The devices were installed one by one at the measurement point. Wave measurements began on 09 July 2015 at 21:12 and ended on 10 May 2017 at 23:01, while the length of the time series was 700 days. The accuracy of measuring bottom hydrostatic pressure, which was subsequently converted into sea level oscillations (waves) taking into account the attenuation of short waves with depth, is 0.06% of the full scale, and the pressure resolution is ±0.0003% also of the full scale. The measurement discreteness is 1 s. Wind and atmospheric pressure data are taken from the open "Weather Schedule" website [*Weather Schedule LLC*, 2023] for the Sakhalin region, Korsakovsky district, Okhotskoe. Unfortunately, the weather data in the settlement Lesnoye that close to Okhotskoe began to be registered only from March 2016. Maps of the region and the water area of the installation of devices are shown in Figure 1. The location of devices is shown by a black circle.

Spectral analysis, filtering, subtraction of tides and visualization of results and time series were performed by the Kyma program designed for complex processing and analysis

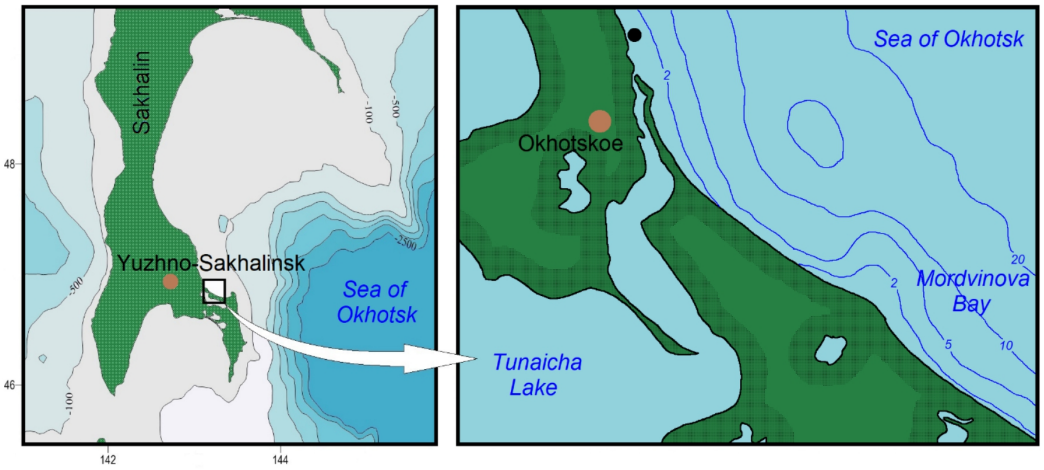

Figure 1. Maps of the region and the water area of the instrument installation. The location of the production is shown by a black circle.

of large-volume sea level data [*Kovalev*, 2018; *Plekhanov and Kovalev*, 2016]. The program allows to calculate the spectral density of sea level oscillations for a selected time series using the usual windowed Fourier transform. The time series is divided into $2n/w - 1$ windows, where n is the length of the time series, w is the size of the window, and the next segment of the series is selected with an offset of half the window length. Each segment is filtered by a Kaiser-Bessel window (filtering can be disabled). Then, for each window, the Fourier transform is calculated for a given number of frequencies, starting from a given frequency. After calculating the spectral parameters for each window, the average value between them is calculated.

To remove astronomical tidal fluctuations and shorter waves in the analysis subtidal periods, a digital low-pass filter was used to remove oscillations with periods shorter than 30 hours. The check showed that the restriction on this period is quite sufficient, although in the studies [*Andrade et al.*, 2018] a filter with a period of 40 hours was used.

As a result of the observations, a long-term time series was obtained, shown in Figure 2a. The same figure shows a time series with filtered oscillations, periods of which are shorter than 30 hours (Figure 2a, highlighted in blue) and a series containing wind waves, swell and short IG waves with periods up to 10 minutes (Figure 2b), which allows us to judge about the state of the sea surface for the entire observation time.

From Figure 2b clearly shows that at the moments when the sea is covered with ice from February to April, sea level fluctuations due to the impact of winds are minimal, although for these moments in the time series for wave periods of more than 30 hours, significant variations in sea level are nevertheless present. This indicates that there are variations in sea level, caused not only by the impact of winds and storm waves.

3. Astronomical Tidal Level Oscillations

A long time series of observations of sea level oscillations makes it possible to calculate the periods of the main astronomical tidal harmonics more accurately than in previous studies, for example, those described in the paper [*Kovalev et al.*, 2021]. The periods of these harmonics are determined from the spectral densities of sea level oscillations calculated using the Kyma program [*Kovalev*, 2018]. To confirm that these periods are astronomical, the spectral density is calculated from the time series, from which the precalculated astronomical tide is subtracted and the spectral densities are compared. Calculation of tidal harmonics and their subtraction from the original time series is performed using 35 astronomical harmonics using the `LSMTM.exe` application in the Kyma program.

Figure 3 shows the spectral densities of sea level oscillations calculated from the time series with the tide (curve line 1) and the time series from which the precalculated

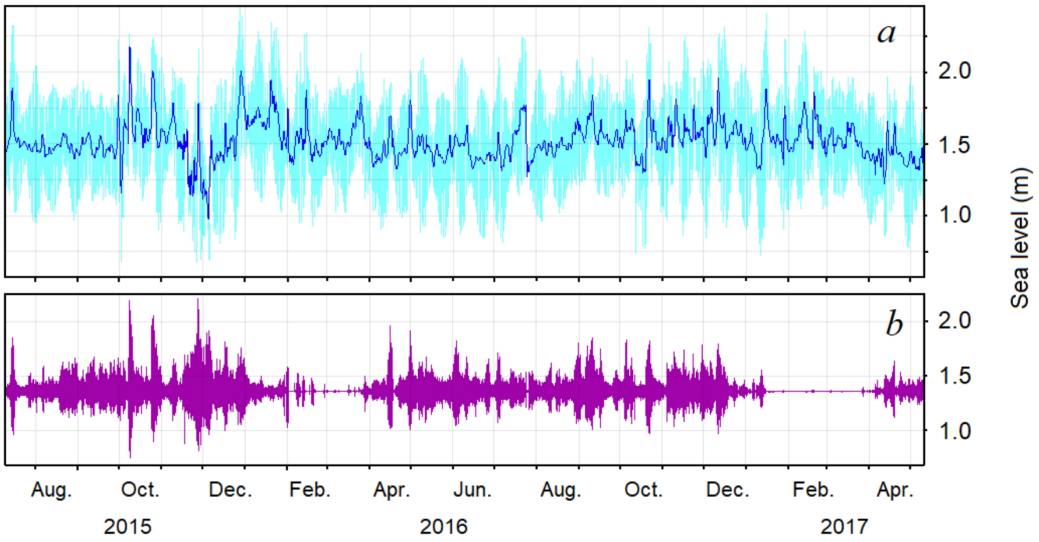

Figure 2. The original time series of sea level oscillations with tide (light tone) and level variations for periods longer than 30 hours, highlighted in blue (a), short-period waves up to 10 minutes (b).

astronomical tide is subtracted (curve line 2). A comparison of spectral densities shows that significant peaks correspond to astronomical tidal harmonics. It is also seen that there are tidal harmonics up to periods of about four hours. The peak periods in spectral densities and their correspondence to astronomical tidal harmonics are shown in Table 1.

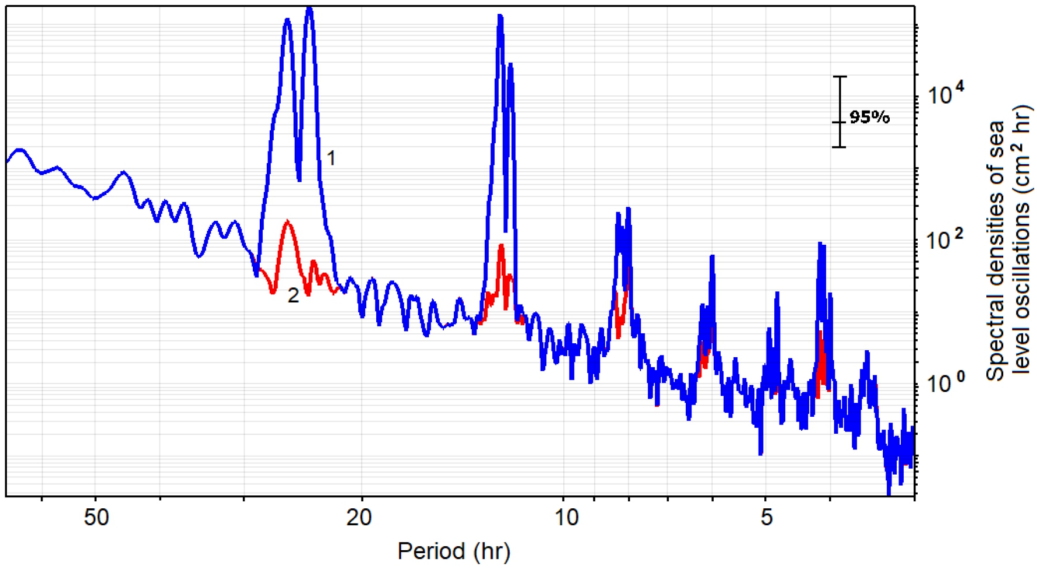

Figure 3. Spectral densities of sea level oscillations calculated from the original time series with the tide (1) and the time series from which the precalculated astronomical tide (2) is subtracted.

According to the calculated spectral density of sea level oscillations shown in Figure 3, the amplitudes of tidal harmonics shown in Table 1 are calculated. The average amplitude of oscillations at a given frequency (period) was determined by the formula:

$$\bar{A}^2 = \int_{\omega_1}^{\omega_2} S(\omega) d\omega, \tag{1}$$

where integration was carried out over the frequency interval, in the vicinity of the peak. In addition, for verification purposes, the amplitudes of tidal harmonics were determined using the Kyma program, which made it possible to identify individual wave processes with specific periods. The results obtained in both cases turned out to be close. In the studies given in the monograph [*Kovalev and Shevchenko*, 2008] The calculation was also performed using formula (1) and confirmed the possibility of such determination of the amplitudes of tidal harmonics.

Table 1. Peak periods in spectral densities and their correspondence to astronomical tidal harmonics

	Peak period in spectral density (hr)											
Time series with the tide	25.83	23.98	12.43	12.00	8.28	8.17	8.00	6.00	4.80	4.13	4.08	4.00
Harmonic [*Parker*, 2007]	M_1	K_1	M_2	S_2	M_3	MK_3	SP_3	S_4	$3KM_5$	M_6	$2MK_6$	S_6
Harmonic amplitude (cm)	33.0	43.0	18.0	8.9	3.1	3.1	2.9	1.6	1.0	2.2	2.4	1.0

The obtained values of tidal harmonic amplitudes allow one to calculate the form number N_f using the equation [*de Miranda et al.*, 2002]:

$$N_f = (K_1 + M_1)/(M_2 + S_2),$$

where K_1, M_1, and M_2, S_2 are the amplitudes of the main diurnal and semidiurnal tide harmonics, respectively. This number determines the relative contribution of the diurnal and semidiurnal components, and the tidal regime in each water area can be determined following the classification proposed in the paper [*de Miranda et al.*, 2002]. For the water area under consideration, in accordance with the data in Table 1, $N_f = 2.8$. Then the tide is classified as mixed with a predominance of diurnal since it falls in the range of values $1.5 < N_f < 3.0$ [*de Miranda et al.*, 2002].

4. Long-Term Sea Level Variations of Non-Astronomical Nature

Prolonged ascents and descents in the level can be associated with changes in atmospheric pressure and effects of wind resulting from the aerodynamic roughness of the sea surface and the transmission of turbulent momentum transfer. There are various techniques for determining the momentum transfer such as the geostrophic departure, aerodynamic (profile) and the eddy correlation methods [*Sudolsky*, 1991].

The influence of pressure at the open boundary is taken into account by correcting the open boundary condition using the concept of an "inverted barometer":

$$\Delta\zeta = -\frac{1}{\rho_w}(p - \bar{p}),$$

where $\bar{p} = 1012\,\text{hPa}$, ρ_w is the density of water, p is the atmospheric pressure at sea surface.

The wind stress $\vec{\tau}$ is calculated from the wind speed at a 10-meter height $\vec{\mathbf{u}}_{10}$ in accordance with the ratio:

$$\vec{\tau} = \rho_a C_D |\vec{\mathbf{u}}_{10}| \vec{\mathbf{u}}_{10},$$

where ρ_a is the air density, for which a constant value of 1.205 kg m^{-3} is assumed. The coefficient of aerodynamic drag C_D is determined by the equation:

$$C_D = \left(\alpha + \beta |\vec{\mathbf{u}}_{10}|\right)/10^3, \quad (2)$$

with constants $\alpha = 0.63$ and $\beta = 0.066$ [*Jones and Toba*, 2001].

An assessment of the relative importance of the effects of wind stress and atmospheric pressure is provided by analyzing the order of magnitude of these two terms in the

horizontal momentum transfer equations. And depending on the water depth h, the Coriolis frequency f, the ratio of pressure to wind action is determined by the formula [*de Vries et al.*, 1995]:

$$\alpha^* = \frac{hf}{C_D u_{10}}.$$

The values of the aerodynamic drag coefficient calculated using equation (2) for the edge values of the wind speed range 3 and 9 m s^{-1}, at which significant variations in sea level were observed, showed 0.828×10^{-3} and 1.22×10^{-3}. They are close to the obtained value $C_D = 1.42 \times 10^{-3}$ in the paper [*Jones and Toba*, 2001]. For the obtained C_D values, the estimates of the relative significance of the effects of wind stress and atmospheric pressure are 6.7 and 1.5, respectively. And since $\alpha^* > 1$ in the Sea of Okhotsk, storm surges on the basin scale for such α^* values imply a predominance of atmospheric pressure, while for seas with $\alpha^* < 1$ it is assumed that storm surges in this water area are influenced by wind [*de Vries et al.*, 1995].

Although α^* estimates are useful for obtaining an accurate value of atmospheric pressure over wind-dominated seas, there may be many potentially important exceptions associated with variations in sea depth and surges caused by atmospheric pressure gradients over a deep water area that may extend into shallow waters [*Timmerman*, 1975].The relative humidity of wind and pressure may depend on the orientation of the isobars and the direction of storm propagation also [*de Vries et al.*, 1995], which are not considered here.

When studying the impact of meteorological factors on sea level changes, it is necessary to consider the rotation of the Earth, which can be estimated using the Kelvin number β, for the mode of longitudinal oscillations of an open basin, which is determined by the ratio of the width of the basin W to the Rossby radius R [*Gill*, 1982],

$$\beta = \frac{W}{R} = \frac{fW}{\sqrt{gh}},$$

where $g = 9.81$ m s^{-2} is the acceleration of gravity. The calculated estimates of β obtained for the southern part of the Sea of Okhotsk, taking into account depth variations, showed values not exceeding 0.98. Considering that rotation is especially important for values $\beta > 1$ [*de Vries et al.*, 1995], rotational effects are less significant for the Sea of Okhotsk. Here the length of the basin $L > W$ and a larger Kelvin number are obtained for transverse vibrational modes.

5. Sea Level Rise Events

To study long waves and sea level rises based of non-astronomical nature, the original time series was filtered out with a low-pass digital filter for periods longer than 30 hours.

The resulting series is shown in Figure 4a. Since the mechanism of excitation of long waves considered here is atmospheric disturbances, according to the open "Weather Schedule" website [*Weather Schedule LLC*, 2023] the time series of the wind speed vector modulus (Figure 4b), atmospheric pressure fluctuations (Figure 4d) were used, as well as a time diagram of the winds (Figure 4c). These observations were carried out in the settlement Lesnoye, located on the coast at a distance of 7.5 km from the installation site of the wave meter. Unfortunately, meteorological observations began here only at the end of February 2016.

Table 2 shows the events for the maximum sea level rise associated in time with the maximum wind speed or minimum atmospheric pressure. All increases in the sea level associated with the impact of winds on the sea surface are observed when the winds are directed north, and a decrease in the sea level is observed when the winds are directed south. This is explained by the fact that northern winds create a storm surge in the coastal zone of Mordvinov Bay, since the shore creates an obstacle to the surge currents, and southern winds create a downsurge near the coast where the device was installed. With an average sea level of 152 cm during the period when meteorological observations were

carried out from February 2016 to May 2017, the maximum rise in sea level was 31 cm, and the decrease was 20 cm.

It should be noted that according to the instructions of the Russian Federal Service for Hydrometeorology and Environmental Monitoring dated August 23, 2002, upsurge-downsurge phenomena are classified as dangerous marine hydrometeorological phenomena [*Kovalev*, 2013]. And although in the studied water area the maximum height of the storm surge wave turned out to be small, but together with the astronomical tide, the amplitudes of the main harmonics of which reach 43 cm, the total rise in sea level can pose a danger in the coastal zone.

There is one more remark regarding the analyzed sea level rises associated with the impact of wind on the sea surface. Some of the sea level rises coincide in time with the level rises caused by changes in atmospheric pressure. These include the events of 15 and 30 April 2016. This happens for obvious reasons – both winds and changes in atmospheric pressure are observed when atmospheric disturbances pass over the observation area, therefore at such moments, when the conditions from the impact of wind and atmospheric pressure coincide, sea level rises are recorded.

Table 2. Sea level rises are associated with the impacts of wind and atmospheric pressure

Wind impacts sea level				Atmospheric pressure impacts sea level			
Date	Time of maximum	Wind speed ($m\,s^{-1}$) and direction	Sea level (cm)	Date	Time of maximum	Atmospheric pressure (mm Hg)	Sea level (cm)
15 Apr. 2016	16:57	20 N	170	14 Feb. 2016	18:22	745	186
30 Apr. 2016	14:04	17 N	180	15 Apr. 2016	16:57	752	170
10 June 2016	20:06	14 N	163	30 Apr. 2016	14:04	749	180
10 Sept. 2016	05:34	16 N	183				
13 Apr. 2017	14:11	14 N	166				

It should be noted that it is almost impossible to visually assess correlation or coherence using time series of sea level and atmospheric pressure oscillations. It is well known, for example, [*Rabinovich*, 1993], that energy from atmospheric disturbances is transferred to sea waves mainly in a complicated way. But already a comparison of the spectra shows the connection between sea level oscillations and changes in atmospheric pressure. The graphs of the spectral densities of sea level and atmospheric pressure oscillations in Figure 5 show the coincidence of the periods of some peaks and at these periods resonant energy transfer is possible. It is not possible to calculate the cross spectrum or coherence since the atmospheric pressure data were measured only twice a day and therefore the small number of reports for the entire time series, only about 600.

6. Events With a Decrease in Sea Level

In addition to prolonged sea level rises, many events with a decrease in sea level were also noted, which are shown in the Table 3. To analyze the conditions of decrease in the sea level, graphs of wind speed, duration of its impact and the magnitude of sea level decrease were plotted, which are shown in Figure 6. The graph of atmospheric pressure changes is not given, since its change does not exceed 2% and looks like a straight line.

From Figure 6 shows that the magnitude of the sea level decrease for events 5 and 10, for which higher wind speeds and durations of impact to westerly winds are correlated. The wind speed has less effect on the magnitude of the sea level decrease than its duration. So, for event 4 of 06 July 2016, despite the high wind speed, with the duration of its impact for two days, the sea level decrease is 22 cm, while for event 5, with a lower wind speed, the sea level drop is 25 cm.

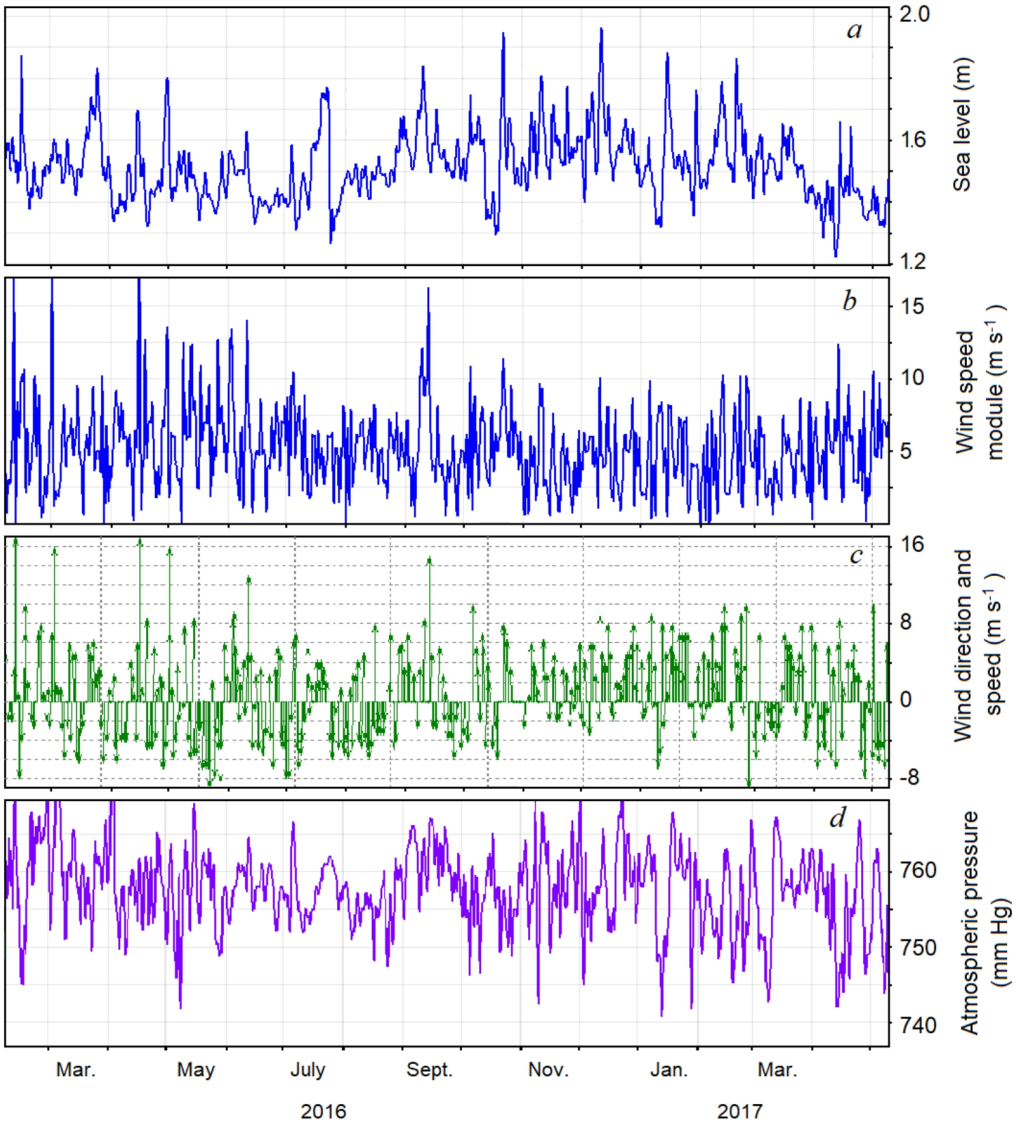

Figure 4. The time series of sea level oscillations, after filtering the original time series with a low-pass filter with a cutoff period of 30 hours (a), wind speed module (b), wind direction and speed, positive direction – north wind (c), atmospheric pressure fluctuations (d).

Note that the duration of the detected sea level decreases is close in duration to the previously observed downsurges of 1–2 days. Such downsurge phenomena for the open sea are described in the papers [*Kato et al.*, 2003; *Kovalev*, 2013]. Therefore, considering all the circumstances, namely the duration of the events, the presence of westerly winds allows us to make a conclusion similar to that given in these papers that the sea level decreases under consideration are downsurges due to the impact of winds.

7. Sea Level Rises Associated with Decreased Atmospheric Pressure

Table 2 shows the events in which sea level rises are observed associated with a decrease in atmospheric pressure. At the same time, the increase in sea level from the average sea level is from 14 to 35 cm with a decrease in atmospheric pressure by 9–15 mmHg (12–20 hPa). Further calculations and analysis showed that these events can be attributed to a phenomenon with the "inverted barometer" law. In other events not included in Table 2, sea level rises were less than 14 cm with a decrease in atmospheric pressure of less than 9 mmHg, or were not associated with a decrease in atmospheric pressure.

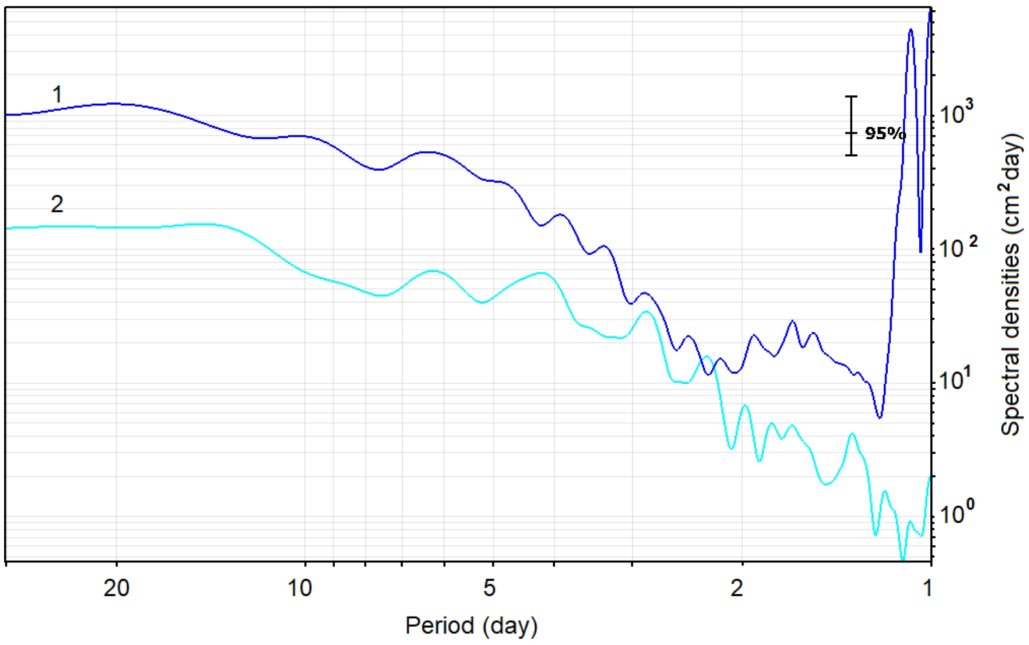

Figure 5. Spectral densities of sea level (1) and atmospheric pressure (2) oscillations.

Table 3. Events with a decrease in sea level

Event	The date of the minimum sea level	Time	Sea level (cm)	The duration of the decrease from the average daily level (day)	Atmospheric pressure (mmHg)	Wind ($m\,s^{-1}$), direction	The duration of the wind (day)
1	03 Apr. 2016	15:07	134	2.5	755	7–9 SW	1,5
2	20 Apr. 2016	20:33	132	2	758	5–7 S, SW	2,5
3	15 June 2016	07:12	132	3	758	4–5 SW, S	2
4	06 July 2016	9:08	130	1.7	761	5–9 S	2
5	24 July 2016	19:35	127	1	763	6 -7 SW	3
6	14 Oct. 2016	12:06	135	0.5	762	3 S, SW	3
7	18 Oct. 2016	10:24	130	2	756	5–6 S, W	2
8	10 Jan. 2017	13:36	132	1	750	1–8 SW	3
9	29 Jan. 2017	04:06	135	1.5	750	3–4 W, SW	2
10	11 Apr. 2017	16:50	122	1.5	750	5–7 SW, S	3

The mechanism of action of the "inverted barometer" law can be explained from the hydrostatic equation relating atmospheric pressure P_a and sea level rise η, which is written in the following form [*Ponte*, 2006]:

$$P = \rho g(z + \eta) + P_a, \tag{3}$$

where $\rho = 1025\,kg\,m^{-3}$ is the density of water, z is the distance from the sea surface. And for the steady-state equilibrium position, $\eta^* = -P_a/\rho g$ will be executed. It can be seen that a decrease in atmospheric pressure will cause an increase in the sea level. And to assess the reaction of sea level to changes in atmospheric pressure, the spatial and temporal scales of

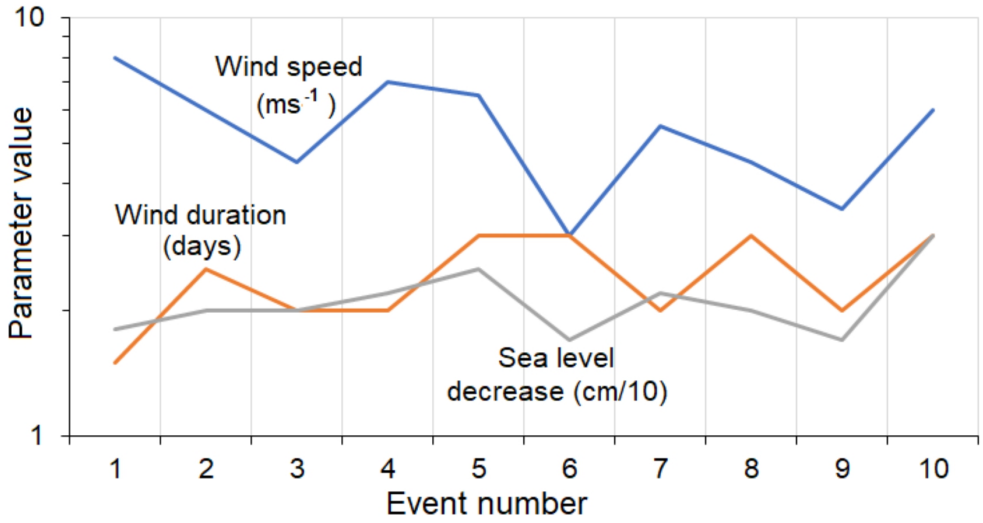

Figure 6. Values of wind speed, duration of its influence and the magnitude of the sea level drop.

which correspond to normal weather systems a barometric coefficient was introduced, the theoretical value of which is close to -1.01 cm mbar^{-1} [*Wunsch and Stammer*, 1997].

Note that the simple equation (3) is a rough approximation of the "inverted barometer" law, it does not consider the speed of propagation of atmospheric disturbances. And to calculate the sea level response to changes in atmospheric pressure, it is necessary to use the equation:

$$\Delta\eta = -\Delta P_a / \left[\rho g (1 - c^2/gH)\right],$$

where c is the speed of atmospheric disturbance propagation, H is the depth of the sea.

Calculations for the observed speeds of cyclones movement for the studied observation area, which are usually in the range of 15–30 knots (7.7–15.4 m s^{-1}) [*Kovalev et al.*, 2022] showed that the magnitude of sea level rise for the observed range of atmospheric pressure changes of 12–20 hPa is from 20 to 33 cm. These values are close to the observed sea level rises for the events shown in the Table 2.

Extensive studies on the inverted barometric or "isostatic" response are described in the paper [*Hamon*, 1966]. Observations of daily changes in sea level and atmospheric pressure were carried out using 17 tidal stations located on the coast of Australia. To analyze the main features of the change in the barometric factor (regression coefficient), the regression of the average daily sea level to the average daily atmospheric pressure was used. Here we also calculated the regression coefficient for sea level rise events associated with a decrease in atmospheric pressure, shown in Table 2.

The average daily value of sea level was calculated from the data of the original time series, from which the Kyma program subtracted the precalculated tide and then calculated the average values over four-hour segments and determined the values of sea level increments, from which the average daily value of sea level change was calculated. The average daily change in atmospheric pressure was calculated similarly using the average values of four-hour changes. Then, using the obtained average daily values, regression coefficients were calculated. The obtained values are shown in Table 4.

According to research data [*Isozaki*, 1969], the relationships between the daily change in sea level and the change in atmospheric pressure were obtained for 53 tidal stations on the coast of the Japanese islands. The calculated values of the regression coefficient are close to the theoretical value (-1.01 cm mbar^{-1}) for many stations on the coasts directly facing the open ocean. At the same time, as can be seen from Table 4, the parameter values for different sea level rise events due to the "inverted barometer" law differ significantly and the modulus of the regression coefficient is significantly greater than the theoretical

one. Similar values of the regression coefficient for some stations were obtained in the studies of B. V. Hamon [*Hamon*, 1966].

Table 4. The values of changes in atmospheric pressure, sea level and regression coefficients for sea level rise events in connection with the "inverted barometer" law

Parameter \ Event	14 Feb. 2016	15 Apr. 2016	30 Apr. 2016
Maximum four-hour change in atmospheric pressure (hPa)	3.9	2.9	2.3
Maximum sea level change in four hours (cm)	10.6	5.27	2.7
Regression coefficient ($cm\,hPa^{-1}$)	−2.68	−2.23	−1.49

Note: since all regression coefficient values are calculated using six values, the value of the confidence criterion for them, calculated using the Student's table for probability 0.9, is 2.015.

Based on the available data, in these studies concluded that traveling continental shelf waves exist all times on the east and west coasts of Australia. These traveling waves are probably energized by atmospheric pressure variations. The traveling wave hypothesis is supported by delays observed between sea levels at neighboring stations. At the same time, the phase relations are such that traveling waves seem to reduce the direct reaction of sea level to atmospheric pressure on the east coast and increase the reaction on the west coast. The same conclusion can be attributed to the studies described here.

The shelf waves that are referring to B. V. Hamon, are formed as a result of the combined effect of the variability of the seabed relief and the rotation of the Earth. They are a consequence of the law of conservation of a potential vortex. These waves are generally thought to be generated by atmospheric forcing or wind [*Brunner et al.*, 2019], but authors of paper [*Darelius et al.*, 2009] suggest the possibility of other generation mechanisms, such as interactions between currents and topography.

In general, the conditions for the excitation of shelf waves in areas where the direction of their propagation coincides with the direction of movement of atmospheric disturbances are more favorable than where these directions are opposite. However, even in the latter case, shelf waves can be excited due to the scattering of the meteorological tide on the inhomogeneities of the relief [*Brunner et al.*, 2019].

It should be noted that shelf waves are much better manifested in currents than in the sea level – oscillations in the ocean level of several centimeters correspond to currents with speeds of tens of centimeters per second [*Rabinovich*, 1993]. Therefore, in the spectra of sea level oscillations, these waves do not have significantly pronounced maxima, the level rise is small, and an 80% confidence interval is considered here.

A detailed analysis of the spectra of sea level oscillations for periods longer than 24 hours showed the presence of three peaks slightly exceeding the 80% confidence interval for periods of 30.7, 36.2 and 45.1 hours. It was taken into account that the latitude of the installation site of the devices is 46.87°, the inertial frequency is determined by the well-known formula $f = 2\Omega \sin\phi$, where ϕ is latitude, $\Omega = 7.2921 \times 10^{-5}$ cycle s^{-1} is the circular frequency of the Earth's rotation. The value of the $\sin\phi$ function is 0.7298 and taking this into account, we obtain an inertial frequency of 0.383 cycles per hours and the period of inertial oscillations is 16.4 hours. Note also that shelf waves exist at frequencies below the inertial frequency $\omega < f$ [*Rabinovich*, 1993]. Considering that the period of the observed waves is more than 16.4 hours, the detected wave processes can be attributed to offshore waves.

Using the dispersion relation for waves of the continental shelf obtained by Buchwald and Adams [*Adams and Buchwald*, 1969], a dispersion diagram of shelf waves was calculated (it is not presented) for the exponentially profile of the seabed on the shelf in the area of instrument installation, which showed that for the detected wave periods of 30.7, 36.2 and 45.1 hours, the existence of the first four modes of shelf waves is possible. Therefore, we

can assume that B. V. Haman's conclusion about the influence of shelf waves on sea level rises and, as a result, on the value of the regression coefficient is valid.

8. Wave Set-Up

The above analysis of events of sea level changes associated with meteorological reasons showed that the total number of events with an ascent and descent in sea level for the period from April 2016 to May 2017, when meteorological observations were carried out, amounted to 31 events, of which eight sea level ascents associated with the impact of wind, ten with descents in sea level and three are caused by the "inverted barometer" law. The remaining 10 events also correspond to sea level rises from an average height of up to 23 cm.

The explanation of the physical mechanism of wave set-up formation was first proposed by *Longuet-Higgins and Stewart* [1962, 1964]. They developed a model of this phenomenon and showed that the wave set-up is formed by horizontal gradients of radiation stress. Introduced by Longuet-Higgins and Stewart, the term "radiation stress", in their understanding, means an excess of momentum transfer caused by the translational movement of wind waves.

A generalization of the Longuet-Higgins-Stewart theory for arbitrary depth relief in the surf zone was made by *Leontiev* [1980]. He obtained an equation connecting the height of the wave set-up with the wave parameters at the moment of breaking:

$$\tilde{\zeta} = \frac{1}{8} k_H \gamma_b^2 h_b,$$

where $\gamma_b = H_b/h_b$ is the relative height of the waves at the moment of breaking, h_b is the depth of the beginning of the breaking, H_b is the height of the breaking waves. The k_H coefficient is a characteristic of the bottom profile in the surf zone and is determined by the equation:

$$k_H = \sqrt{\frac{h_b}{\bar{h_b}(x)}},$$

here $\bar{h_b}$ is average depth along the surf zone. For a flat inclined bottom $k_H = 3/2$ and the level rise is

$$\tilde{\zeta} = 3.16 \gamma_b^2 h_b, \tag{4}$$

which corresponds to the theoretical results of *Longuet-Higgins and Stewart* [1962].

The values of the wave set-up heights calculated using equation (4) for waves with a weak storm with a wave height of up to 42 cm and for moderate storms with a wave heights of up to 78 cm noted during the observation period range from 11 cm to 38 cm. They correspond in time to the existence of storm waves, which can create a wave set-up within the obtained values. This additive, even with an average storm wave size and when coinciding in time with a K_1 tide with a height of 43 cm, a storm surge of 31 cm and an ascent in the sea level to 34 cm associated with a decrease in atmospheric pressure, can lead to a rise in the sea level to 125 cm, with a maximum estimate of 146 cm. Such values of sea level rise are catastrophic and lead to floods [*Kato et al.*, 2003].

Note that the wave height estimates used above were obtained from devices installed in a sufficiently closed basin near the settlement Okhotskoe, that weakens wind waves and swells. For the open coast south of the settlement, the wave heights in the breaking area often reaches 1.2 m, and in a very strong storm, waves up to 3.4 m high can be observed (September 13, 2021). Naturally, the magnitude of the wave set-up in these cases will be greater and for 1.2 m waves will be 0.46 m.

9. Sea Level Rise Profiles

In the paper [*Squire et al.*, 2021b], the profiles of storm surge waves were considered. These waves were described using the profile of a cnoidal wave. It is of interest to check whether same profiles are observed for the sea level rises analyzed here, which can be

considered as single waves, representing the limiting case of a cnoidal wave – a long, nonlinear surface gravitational wave with a relatively sharp crest. In fluid dynamics, a cnoidal wave is a nonlinear and accurate periodic wave solution of the Korteweg–de Vries equation (KDV) [*Dingemans*, 1997; *Osborne*, 2002]. Let's consider the model profile of such waves and compare it with the waves of storm surges and sea level rises associated with atmospheric pressure.

The KDV equation can be given in dimensionless variables, as for example in [*Hereman*, 2009]:

$$u_t + \alpha u u_x + u_{xxx} = 0, \tag{5}$$

where indices denote partial derivatives. The nonlinearity coefficient α can be scaled to any real number [*Hereman*, 2009] usually use the values $\alpha = 1$ or $\alpha = 6$.

The term u_t describes the temporal evolution of a wave propagating in one direction, and equation (5) is called the evolutionary equation. The nonlinear term $\alpha u u_x$ describes the steepness of the wave, and the linear dispersion term u_{xxx} describes the propagation of the wave.

Korteweg and de Vries [1895] showed that equation (5) also has a simple periodic solution,

$$u(x,t) = \frac{\omega - 4k^3(2m-1)}{\alpha k} + \frac{12k^2 m}{\alpha} cn^2(kx - \omega t + \delta; m),$$

which they called the cnoidal wave solution because it involves the cn-elliptic Jacobi cosine function with the ellipticity parameter m ($0 < m < 1$). The wave number k in this case determines the period of the cnoidal wave.

Based on field data, profiles of sea surface elevation are recorded depending on time, therefore, to compare them with the theoretical profile calculated using the KdV equation, it is advisable to use the time form of this equation, denoted as the TKdV equation (T – means the time form of the equation) [*Osborne*, 2002]. The approximate soliton solution of such an equation has the form [*Giovanangeli et al.*, 2018]:

$$\eta(x,t) = A \operatorname{sech}^2 \frac{t - x/V}{T}, \tag{6}$$

where η is the elevation of the surface, the speed V and duration T are related to the amplitude A:

$$V = \frac{c_0}{1 - c_0 A/3} \approx c_0\left(1 + \frac{c_0 \alpha A}{3}\right), \qquad T = \sqrt{\frac{12\beta}{\alpha A}},$$

where $c_0 = (gh)^{1/2}$, $\alpha = 3/(2c_0 h)$, $\beta = h^2/(6{c_0}^3)$ is dispersion coefficient, g is the acceleration due to gravity and h is the unperturbed water depth. This approximate formula is valid for small amplitude solitons at $c_0 \alpha A/3 \ll 1$.

For the measured sea level elevations shown in the Table 2, containing storm surges and level rises associated with atmospheric pressure, graphs of normalized amplitudes are plotted together with a model profile calculated using TKDV (6), shown in Figure 6. The following parameter values were used in the calculations: $T = 45 \times 10^3$ s, $A = 0.1$ m, $h = 1.5$ m, $x = 14 \times 10^5$ m.

Figure 7 shows that the model profile is close in shape to the observed profiles. At the same time, the two profiles 5, 6 are significantly narrower than the theoretical one. These profiles relate to level rise events caused by various causes – wind impact and a decrease in atmospheric pressure. An analysis of the possible reasons for such a difference between these two profiles from the rest showed that the maximum increase in the level on 14 February 2016 (profile 5) coincided with the maximum of the spring tide, and since the duration of the increase is usually about two days, and the daily tidal harmonic is about two times less, then as a result of the joint influence, a "narrowing" of the profile of sea surface rise is possible. A similar situation was observed for an increase in the sea level on

13 April 2017 (profile 6), while the magnitude of the sea level change due to wind impact was small.

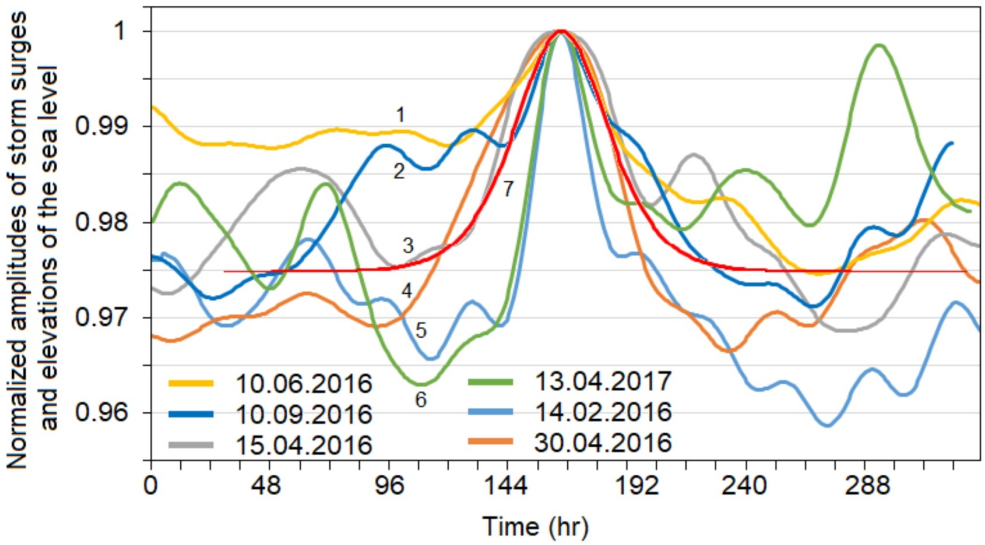

Figure 7. Normalized amplitudes of storm surges (lines 1, 2, 3, 4, 6) and elevations of the sea level due to a decrease in atmospheric pressure (lines 3, 4, 5), combined with the theoretical profile (line 7).

It should be noted that there could be two reasons of manifestation for each of the observed two sea level elevations on April 15 and 30, 2016. They were accompanied by both strong winds and low atmospheric pressure. It was not possible to establish what was decisive for the change in the level, and possibly the joint impact, within the framework of this paper. But, considering all the circumstances discussed above, it can be concluded that the profiles of the considered sea level elevations and storm surge waves are well described by the profile of a single cnoidal wave.

10. Conclusions

The study of tidal and subtidal variations in sea level in the area of the southeastern coast of the Sakhalin Island was carried out according to a time series of 700 days measured with a second discreteness. At the same time, the analysis of the relationship between sea level variations and meteorological conditions was carried out using time series duration about 15 months due to the lack of meteorological observations in the studied area in the previous period.

The study of astronomical tides in the water area under consideration was carried out using spectral analysis. Diurnal M_1, K_1 and semidiurnal M_2, S_2 tidal harmonics with high energy have been detected. For other harmonics, the wave energy is three orders of magnitude less. The maximum heights of tidal waves have been determined, the maximum of which for K_1 is equal to 43 cm. It is shown that the form number determining the relative contribution of diurnal and semi-diurnal components is 2.8 and this makes it possible to classify the tidal regime in this region as mixed with a predominance of diurnal.

Long-term changes in sea level variations associated with meteorological conditions were studied. It is shown that the sea level rises caused by the impact of winds on the sea surface are observed when the winds are northerly, and level decreases are observed when the winds are southerly. This is due to the fact that northern winds create a storm surge in in the coastal zone of Mordvinov Bay, since the coast creates an obstacle in the way of surging currents, and southern winds create a downsurge near the coast where the wave meter is installed.

During the observations, many events with a decrease in sea level were detected for wind speeds from 3 to 9 m s^{-1}. It is shown that the magnitude of the sea level decrease

for events in which higher wind speeds and the duration of impact to westerly winds are correlated is maximal, and the wind speed has less influence on the magnitude of the level decrease than its duration. The duration of the detected decreases in sea level is close to previously observed storm surges of 1–2 days, described in published papers.

The events with sea level rises associated with a decrease in atmospheric pressure are considered. Calculations of the sea level response to changes in atmospheric pressure using the Proudman equation, and analysis of the results showed that these events can be attributed to events with the "inverted barometer" law. The calculated values of the regression coefficients for these events showed values 1.5–3 times higher than the theoretical ones. Research by Hamon (reference) showed that such differences in the regression coefficient from the theoretical one may be associated with the waves of continental shelf.

A detailed analysis of the spectra of sea level oscillations over the original time series for periods longer than daily showed the presence of three peaks exceeding the 80% confidence interval for periods of 30.7, 36.2 and 45.1 hours. The calculation of the dispersion ratio for waves of the continental shelf for exponentially profile of the seabed on the shelf in the area of installation of devices showed the possibility of the existence of shelf wave modes on these periods. Based on this, taking into account the conclusion of B. V. Hamon, it is possible to assume the influence of shelf waves on sea level rises and, as a result, on the value of the regression coefficient.

The sea level increases associated with wave set-up, which can be essential and significantly affect the variability of sea level in the coastal zone, are considered. The explanation of the physical mechanism of this phenomenon was proposed by Longuet-Higgins and Stewart, who showed that it is formed by horizontal gradients of radiation stress. Calculations using the wave set-up height equation showed values ranging from 11 cm to 38 cm for weak and moderate storms noticed during observations. This additive, even at low wave heights, when coinciding with tide K_1, storm surge and an increase in level associated with a decrease in atmospheric pressure, can lead to a rise in level to 119 cm. This value of sea level rise is catastrophic and leads to flooding.

Modeling of sea level rise profiles was carried out from the limiting case of a cnoidal wave, which is a nonlinear and exact periodic wave solution of the Korteweg–de Vries equation. A comparison of the theoretical profile calculated from the time form of the KDV equation with the averaged recorded profiles of level increases showed that they are well described by the profile of a single cnoidal wave.

Acknowledgments. The reported study was funded by the Ministry of Science and Higher Education of the Russian Federation (project No. FWWM-2024-0002).

References

Adams, J. K., and V. T. Buchwald (1969), The generation of continental shelf waves, *Journal of Fluid Mechanics*, *35*(4), 815–826, https://doi.org/10.1017/S0022112069001455.

Andrade, M. M., E. E. Toldo, and J. C. R. Nunes (2018), Tidal and subtidal oscillations in a shallow water system in southern Brazil, *Brazilian Journal of Oceanography*, *66*(3), 245–254, https://doi.org/10.1590/s1679-87592018017406603.

Brunner, K., D. Rivas, and K. M. M. Lwiza (2019), Application of Classical Coastal Trapped Wave Theory to High-Scattering Regions, *Journal of Physical Oceanography*, *49*(9), 2201–2216, https://doi.org/10.1175/JPO-D-18-0112.1.

Darelius, E., L. H. Smedsrud, S. Osterhus, A. Foldvik, and T. Gammelsrod (2009), Structure and variability of the Filchner overflow plume, *Tellus A*, *61*(3), 446–464, https://doi.org/10.1111/j.1600-0870.2009.00391.x.

de Miranda, L. B., B. M. de Castro, and B. Kjerfve (2002), *Princípios de Oceanografia Física de Estuários*, 152 pp., EDUSP, Sao Paulo.

de Vries, H., M. Breton, T. de Mulder, Y. Krestenitis, et al. (1995), A comparison of 2D storm surge models applied to three shallow European seas, *Environmental Software*, *10*(1), 23–42, https://doi.org/10.1016/0266-9838(95)00003-4.

Dingemans, M. W. (1997), *Water Wave Propagation Over Uneven Bottoms: (In 2 Parts)*, 782 pp., World Scientific Publishing Company, https://doi.org/10.1142/9789812796042.

Gill, A. E. (1982), *Atmosphere-Ocean Dynamics*, 662 pp., Academic Press, London.

Giovanangeli, J.-P., C. Kharif, and Y. Stepanyants (2018), Soliton spectra of random water waves in shallow basins, *Mathematical Modelling of Natural Phenomena*, *13*(4), 40, https://doi.org/10.1051/mmnp/2018018.

Goryachkin, Y. I., V. A. Ivanov, and Y. A. Stepanyants (1999), Oscillations of the Black Sea sea level in the north part of the coast, *Physical Oceanography*, *10*(2), 123–130, https://doi.org/10.1007/BF02512983.

Hamon, B. V. (1966), Continental shelf waves and the effects of atmospheric pressure and wind stress on sea level, *Journal of Geophysical Research*, *71*(12), 2883–2893, https://doi.org/10.1029/JZ071I012P02883.

Hereman, W. (2009), Shallow Water Waves and Solitary Waves, in *Encyclopedia of Complexity and Systems Science*, pp. 8112–8125, Springer New York, https://doi.org/10.1007/978-0-387-30440-3_480.

Isozaki, I. (1969), An Investigation on the Variations of Sea Level due to Meteorological Disturbances on the Coast of Japanese Islands (III): On the Variation of Daily Mean Sea Level, *Journal of the Oceanographical Society of Japan*, *25*(2), 91–102, https://doi.org/10.5928/KAIYOU1942.25.91.

Jones, I. S. F., and Y. Toba (2001), *Wind Stress over the Ocean*, 307 pp., Cambridge University Press, Cambridge, https://doi.org/10.1017/CBO9780511552076.

Kato, L. N., Y. V. Lyubitsky, and G. V. Shevchenko (2003), Assessment of extreme values of sea level fluctuations on the southeastern coast of Sakhalin Island, Sea level fluctuations: collection of papers, in *Sea level fluctuations*, pp. 111–128, Russian State Hydrometeorological University, St. Petersburg (in Russian).

Koohestani, K., Y. Stepanyants, and M. N. Allahdadi (2023), Analysis of Internal Solitary Waves in the Gulf of Oman and Sources Responsible for Their Generation, *Water*, *15*(4), 746, https://doi.org/10.3390/w15040746.

Korteweg, D. J., and G. de Vries (1895), Xli. on the change of form of long waves advancing in a rectangular canal, and on a new type of long stationary waves, *The London, Edinburgh, and Dublin Philosophical Magazine and Journal of Science*, *39*(240), 422–443, https://doi.org/10.1080/14786449508620739.

Kovalev, D. P. (2013), Extreme Negative Surge at the South-Eastern Coast of Sakhalin Island, *Fundamental and Applied Hydrophysics*, *6*(1), 52–56 (in Russian).

Kovalev, D. P. (2018), Patent of the Russian Federation, RU 2018618773, registration date: 07/19/2018, https://new.fips.ru/registers-doc-view/fips_servlet?DB=EVM&DocNumber=2018618773 (in Russian).

Kovalev, D. P., P. D. Kovalev, A. S. Borisov, and K. V. Kirillov (2021), Wave characteristics in the southern part of the Sea of Okhotsk - the area of water transport routes to the southern Kuril Islands, *Geosystems of Transition Zones*, *5*(4), 328–338, https://doi.org/10.30730/gtrz.2021.5.4.328-338 (in Russian).

Kovalev, D. P., P. D. Kovalev, and A. S. Borisov (2022), Long-term rise and fall of level of ice-covered Okhotsk Sea near the coast of Mordvinov Bay, *Journal of Oceanological Research*, *50*(4), 5–29, https://doi.org/10.29006/1564-2291.JOR-2022.50(4).1 (in Russian).

Kovalev, P. D., and D. P. Kovalev (2018), Long-wave processes in southeastern shelf Sakhalin Island, *Ecological Systems and Devices*, *8*, 36–41, https://doi.org/10.25791/esip.08.2018.121 (in Russian).

Kovalev, P. D., and G. V. Shevchenko (2008), *Experimental studies of long-wave processes on the Northwestern shelf of the Pacific Ocean*, 213 pp., Dalnauka, Vladivostok (in Russian).

Kovalev, P. D., A. B. Rabinovich, and G. V. Shevchenko (1991), Investigation of long waves in the tsunami frequency band on the southwestern shelf of Kamchatka, *Natural Hazards*, *4*(2–3), 141–159, https://doi.org/10.1007/BF00162784.

Kurkin, A., D. Kovalev, O. Kurkina, and P. Kovalev (2023), Features of Long Waves in the Area of Cape Svobodny (South-Eastern Part of Sakhalin Island) During the Passage of Cyclones, *Russian Journal of Earth Sciences*, *23*(3), ES3003, https://doi.org/10.2205/2023es000852.

Leontiev, I. O. (1980), On the possibility of forecasting a wave set-up in a surf zone with an arbitrary bottom profile, *Oceanology*, *20*(2), 290–299.

Longuet-Higgins, M. S., and R. W. Stewart (1962), Radiation stress and mass transport in gravity waves, with application to 'surf beats', *Journal of Fluid Mechanics*, *13*(4), 481–504, https://doi.org/10.1017/S0022112062000877.

Longuet-Higgins, M. S., and R. W. Stewart (1964), Radiation stresses in water waves; a physical discussion, with applications, *Deep Sea Research and Oceanographic Abstracts*, *11*(4), 529–562, https://doi.org/10.1016/0011-7471(64)90001-4.

Morozov, E. G., D. I. Frey, A. A. Polukhin, V. A. Krechik, et al. (2020), Mesoscale Variability of the Ocean in the Northern Part of the Weddell Sea, *Oceanology*, *60*(5), 573–588, https://doi.org/10.1134/S0001437020050173.

Osborne, A. R. (2002), Nonlinear Ocean Wave and the Inverse Scattering Transform, in *Scattering*, pp. 637–666, Elsevier, https://doi.org/10.1016/B978-012613760-6/50033-4.

Parker, B. B. (2007), *Tidal analysis and prediction*, NOAA, NOS Center for Operational Oceanographic Products and Services, Silver Spring (Maryland), https://doi.org/10.25607/OBP-191.

Plekhanov, F. A., and D. P. Kovalev (2016), The complex program of processing and analysis of time-series data of sea level on the basis of author's algorithms, *Geoinformatika*, *1*, 44–53 (in Russian).

Ponte, R. M. (2006), Low-Frequency Sea Level Variability and the Inverted Barometer Effect, *Journal of Atmospheric and Oceanic Technology*, *23*(4), 619–629, https://doi.org/10.1175/JTECH1864.1.

Pérez Gómez, B., I. Vilibić, J. Šepić, I. Međugorac, et al. (2022), Coastal sea level monitoring in the Mediterranean and Black seas, *Ocean Science*, *18*(4), 997–1053, https://doi.org/10.5194/os-18-997-2022.

Rabinovich, A. B. (1993), *Long waves of ocean gravity: trapped, resonance and radiation*, 325 pp., Hydrometeoizdat, St. Petersburg (in Russian).

Raj, N., Z. Gharineiat, A. A. M. Ahmed, and Y. Stepanyants (2022), Assessment and Prediction of Sea Level Trend in the South Pacific Region, *Remote Sensing*, *14*(4), 986, https://doi.org/10.3390/rs14040986.

Squire, V. A., D. P. Kovalev, and P. D. Kovalev (2021a), Aspects of surface wave propagation with and without sea ice on the south-eastern shelf of Sakhalin Island, *Estuarine, Coastal and Shelf Science*, *251*, 107,227, https://doi.org/10.1016/j.ecss.2021.107227.

Squire, V. A., P. D. Kovalev, D. P. Kovalev, and V. S. Zarochintsev (2021b), On the trapping of energy from storm surges on the coasts of the Sea of Okhotsk, *Estuarine, Coastal and Shelf Science*, *250*, 107,136, https://doi.org/10.1016/j.ecss.2020.107136.

Sudolsky, A. S. (1991), *Dynamic phenomena in reservoirs*, 262 pp., Hydrometeoizdat, Leningrad (in Russian).

Timmerman, H. (1975), On the importance of atmospheric pressure gradients for the generation of external surges in the North Sea: With plates 5 and 6, *Deutsche Hydrographische Zeitschrift*, *28*(2), 62–71, https://doi.org/10.1007/BF02232250.

Truccolo, E. C., D. Franco, and C. A. F. Schettini (2006), The low frequency sea level oscillations in the northern coast of Santa Catarina, Brazil, *Journal of Coastal Research*, *SI 39*, 547–552.

Valentim, S. S., M. E. C. Bernardes, M. Dottori, and M. Cortezi (2013), Low-frequency physical variations in the coastal zone of Ubatuba, northern coast of São Paulo State, Brazil, *Brazilian Journal of Oceanography*, *61*(3), 187–193, https://doi.org/10.1590/S1679-87592013000300003.

Weather Schedule LLC (2023), Weather Schedule LLC, https://rp5.ru/Weather_in_Sakhalin (in Russian), (visited on 03/31/2023).

Williams, S. J. (2013), Sea-Level Rise Implications for Coastal Regions, *Journal of Coastal Research*, *63*, 184–196, https://doi.org/10.2112/SI63-015.1.

Wunsch, C., and D. Stammer (1997), Atmospheric loading and the oceanic "inverted barometer" effect, *Reviews of Geophysics*, *35*(1), 79–107, https://doi.org/10.1029/96RG03037.